Integrated Network Pharmacology Reveal New Key Curcumin-Binding Targets in Triple-Negative Breast Cancer

Xiaohang Qi
Second Affiliated Hospital of Xi'an Jiaotong University
Hua Zhang
Second Affiliated Hospital of Xi'an Jiaotong University
Shucong Wang
Second Affiliated Hospital of Xi'an Jiaotong University
Lu Qiao
Second Affiliated Hospital of Xi'an Jiaotong University
Li Ma
Xi'an Jiaotong University
Kanghuai Zhang
Second Affiliated Hospital of Xi'an Jiaotong University
Yan Wang
wangyan0819@xjtu.edu.cn

Second Affiliated Hospital of Xi'an Jiaotong University

Research Article

Keywords: natural product, curcumin, triple-negative breast cancer, network pharmacology, molecular dynamics simulation

Posted Date: February 23rd, 2026

DOI: https://doi.org/10.21203/rs.3.rs-8723515/v1

Additional Declarations: No competing interests reported.

Abstract

Purpose: Triple-negative breast cancer (TNBC) is an aggressive malignancy lacking targeted therapies, leading to limited treatment options. Curcumin, a natural polyphenol from Curcuma longa, exhibits promising anticancer activity, but its precise molecular mechanisms and key targets in TNBC remain largely unclear. This study aimed to clarify curcumin's antitumor mechanisms and identify its key targets in TNBC.

Methods: To clarify curcumin's antitumor mechanisms in TNBC, an integrated approach was used, including network pharmacology, molecular docking, 500 ns molecular dynamics simulations, free energy landscape analysis, and MM/PBSA binding free energy calculations.

Results: Network pharmacology analysis identified AURKA, BRAF, and CHEK1 as key genes overlapping between curcumin-associated targets and TNBC-related targets. According to molecular docking, Curcumin displayed favorable binding affinities toward these targets, comparable to reference inhibitors. Stable protein–curcumin complexes with improved conformational stability were shown by molecular dynamics simulations. Strong binding free energies have been identified by MM/PBSA calculations for curcumin–CHEK1 (–209.37 kJ/mol) and curcumin–BRAF (–192.87 kJ/mol), which are similar to inhibitors that have been clinically proven.

Conclusions: Our integrated analysis suggests that curcumin exerts multitarget inhibitory effects in TNBC by concurrently modulating mitotic regulation (via AURKA), MAPK signaling (via BRAF), and DNA damage checkpoints (via CHEK1). Among these, CHEK1 emerged as the most thermodynamically stable and conformationally favorable binding target for curcumin, indicating its potential as a crucial mediator of curcumin's antitumor activity.

1 Background

TNBC is one of the most aggressive subtypes of breast cancer, accounting for approximately 10–20% of all breast cancer cases (Howard & Olopade, 2021). TNBC is characterized by the lack of human epidermal growth factor receptor 2 (HER2), progesterone receptor (PR), and estrogen receptor (ER). As a result, chemotherapy is still the standard treatment for TNBC because hormonal and HER2-targeted treatments don't work (Gupta et al., 2020). Some TNBC subtypes have been granted permits, such as immune checkpoint inhibitors (pembrolizumab, atezolizumab) for PD-L1-positive tumors, PARP inhibitors (olaparib, talazoparib) for BRCA-mutated cases, and the antibody–drug conjugate sacituzumab govitecan for advanced disease (Li et al., 2021). Meanwhile, new targets like epidermal growth factor receptor (EGFR), phosphoinositide 3-kinase (PI3K)/ protein kinase B (AKT)/ mechanistic/mammalian target of rapamycin (mTOR), androgen receptor (AR), and Notch are being studied but are not yet included in standard treatment (Zhu et al., 2023). However, chemotherapy is linked to high toxicity and resistance risk, and the majority of patients still lack access to efficient, clearly defined targeted therapies (Obidiro et al., 2023). This therapeutic gap highlights the pressing need for innovative,

multitargeted approaches that can alter important signaling pathways implicated in the development of TNBC.

Natural products have historically acted as a significant source of anticancer medications owing to their exceptional structural diversity and capacity to interact with many molecular targets (Hashem et al., 2022). This kind of combination makes them very useful for dealing with the complexity and variety of cancer (Naeem et al., 2022). *Curcuma longa*, a member of the ginger family, contains a naturally occurring polyphenolic compound called curcumin in its rhizomes, and underground stems (Kocaadam & Sanlier, 2017). In a struggle against TNBC, curcumin has demonstrated great promise. Curcumin demonstrates strong, multi-targeted anticancer activity against TNBC through altering several signaling pathways, such as PI3K/Akt, Hedgehog/Gli1, JAK/STAT, mTOR, EGFR, and Wnt/β-catenin (Chen et al., 2024; Deng et al., 2022; Farghadani & Naidu, 2021; Li et al., 2022; Liu et al., 2020). Curcumin's therapeutic potential is further enhanced by advanced formulations and when combined with doxorubicin and carboplatin, indicating that it is a promising treatment option for TNBC that awaits clinical validation (Cheng et al., 2021; Dong & Alahari, 2020; G. J. Wang et al., 2022). Although these studies contributed to clarify curcumin's comprehensive anticancer potential, they fail to capture the complex nature of its multi-target mode of action, especially when considering TNBC.

Beyond the conventional "one drug–one target" model, network pharmacology explores compound–target–pathway interactions by combining systems biology and computational pharmacology to find the complex, multiple-target mechanisms of natural compounds (Zhai et al., 2025). It facilitates the development of multi-targeted, synergistic therapies with increased efficacy and safety, speeds up drug discovery, and clarifies mechanisms of action by utilizing big data and computational tools (Noor et al., 2022). However, network-based predictions by themselves frequently are insufficient to verifying the molecular validity of these interactions. Though molecular docking and molecular dynamics (MD) simulations are combined, the predictive effectiveness of docking and MD's capacity to capture flexibility and dynamic stability provide a potent and complementary framework for precisely characterizing ligand–protein interactions (Guterres & Im, 2020). The depth and dependability of structure-based drug discovery are increased by this cooperative method, which also refines binding poses, identifies true binders, and provides comprehensive mechanistic and energetic insights (Trezza et al., 2025).

The current study attempts to offer an organized and mechanistically based comprehension of the potential therapeutic effects of curcumin in TNBC. This study aims to identify new molecular targets and mutation-specific interactions that have not been documented in previous curcumin research, as opposed to concentrating on previously confirmed pathways.

2 Methods

2.1 Identification of Curcumin and TNBC's Potential Targets

The SwissTargetPrediction databases were used to predict curcumin's potential molecular targets (Daina et al., 2019). Meanwhile, the keyword "triple-negative breast cancer" was used to get TNBC-associated genes from the GeneCards databases (Stelzer et al., 2016). Related genes were screened using GeneCards' protein coding categories. We assessed on these datasets on 10 October lastly. The VennDiagram package in R was used to find genes that overlapped between curcumin-related targets and TNBC-associated genes.

2.2 Pathway Enrichment Analysis and Network Construction

To visualize the relationship between curcumin, its predicted targets, and TNBC-related genes, a compound–target–disease (C–T–D) network was built using Cytoscape (v3.10.3) (Shannon et al., 2003).

The STRING database (v12.0) was used to construct the Protein–Protein Interaction (PPI) network of overlapping targets with an interaction confidence score > 0.4 (Szklarczyk et al., 2023). To find hub genes based on topological parameters like degree and betweenness centrality, the generated network was examined using Cytoscape.

To identify enriched biological processes and signaling pathways, functional enrichment analyses were carried out using Metascape (https://metascape.org), including Gene Ontology (GO) and Kyoto Encyclopedia of Genes and Genomes (KEGG) analyses (Zhou et al., 2019). The enrichment parameters were set as Minimum overlap = 3, P-value cutoff = 0.01, and minimum enrichment = 1.5. P-values were adjusted using the Benjamini–Hochberg (BH) method, and terms with adjusted $p < 0.05$ were considered significant

2.3 Selecting Reference Inhibitors and Crucial Targets

AURKA, BRAF, and CHEK1 were chosen as key targets among the identified hub targets due to their high degree centrality within the PPI network and biological significance to TNBC. Using data from AURKA (PDB ID: 5L8L), BRAF V600E (PDB ID: 8C7Y), and CHEK1 (PDB ID: 2YEX), protein crystal structures were acquired from the RCSB Protein Data Bank (PDB) (Iwasa et al., 2025). Positive controls included vemurafenib (BRAF), alisertib (AURKA), and AZD7762 (CHEK1), which are corresponding reference inhibitors. Curcumin's 3D structure was obtained from PubChem (CID: 969516), and Chem3D was used to minimize its energy.

2.4 Docking of Molecular Structure

AutoDock Vina (v1.2.3) with default parameters was used for all molecular docking investigations (Forli et al., 2016). Hydrogen atoms were added, water molecules and unnecessary ligands were eliminated, and Gasteiger charges were assigned using AutoDockTools to create protein structures.

For each protein, the docking grid box was centered at the following coordinates and dimensions:

CHEK1: center (13.8546, 34.7526, 10.2607); box size (25.0 × 25.0 × 25.0 Å)

CCNA2: center (19.361, 0.9451, 5.1374); box size (25.02 × 24.71 × 40.68 Å)

AURKA: center (8.0567, − 14.938, − 19.4916); box size (47.96 × 59.29 × 50.43 Å)

BRAF (V600E): center (− 6.6903, 115.258, 13.0859); box size (53.67 × 48.23 × 49.51 Å)

The energy range was set to 4 kcal/mol, exhaustiveness to 10, and num-modes to 10 for all docking runs. Docking poses were ranked according to binding affinity, and the top-ranked conformation was selected for subsequent molecular dynamics simulations.

PyMOL (v2.5) and Discovery Studio Visualizer 4.5 were used to visualize binding conformations and binding affinities (kcal/mol) (Lashkov et al., 2021).

2.5 Simulations of Molecular Dynamics (MD)

GROMACS (v2020.1) was used to perform 500 ns all-atom MD simulations in order to assess the dynamic stability and binding behavior of the curcumin–protein complexes (GROMACS version 2020.1, 10.5281/zenodo.3685919). Proteins were subjected to the AMBERff19SB force field, while Ligand parameters were generated using the AmberTools23 antechamber module with the AMBER Force Field2 (GAFF2) force field and AM1-BCC atomic charges, water model generated using the TIP3P and using ACPYPE to convert (Sousa da Silva & Vranken, 2012; Tian et al., 2020). Each system, inhibitors, curcumin complex, and apo protein, was neutralized with counterions after being solvated in a TIP3P water box with 8 Å buffering and neutralized with counterions (Na^+/Cl^-). Energy minimization was used to minimize energy until the maximum force was less than 1000 kJ/ mol·nm (1000steps). Subsequently, each system performed 100 ps NVT and NPT equilibrations at 310.15 K and 1 bar. By using the V-rescale thermostat and Parrinello–Rahman barostat with coupling constants of 0.1 ps and 2.0 ps, respectively. Production simulations were run for 500 ns with a 2 fs time step, and trajectories were saved every 10 ps for analysis. All bonds involving hydrogen atoms were constrained using LINCS.

Using common GROMACS tools (including gmx rms, gmx rmsf, gmx gyrate) trajectory analyses were performed to determine the Radius of Gyration (Rg), Root Mean Square Deviation (RMSD), and Root Mean Square Fluctuation (RMSF).

Principal component analysis (PCA) was utilized to build the free energy landscape (FEL) from the MD trajectories in order to investigate conformational stability and energy minima. Reaction coordinates were derived from the first two principal components (PC1 and PC2).

2.6 Binding Free Energy Calculation (MM-PBSA)

By using the g_mmpbsa package, the binding free energies of curcumin with targets were estimated using the Molecular Mechanics Poisson–Boltzmann Surface Area (MM-PBSA) method (Kumari et al., 2014). The total binding energy was expressed as:

$$\Delta G_{bind} = \Delta E_{vdW} + \Delta_{Eele} + \Delta_{Gpolar} + \Delta G_{nonpolar}$$

ΔE_vdW and ΔE_ele are the van der Waals and electrostatic interaction energies, and ΔG_polar and ΔG_nonpolar correspond to the polar and nonpolar solvation energies.

From the representative 100 ns of the trajectories, snapshots were taken every 10 ps. The sum of the solvation free energy components and the molecular mechanics energy (electrostatic + van der Waals) is represented by each term in the calculation of the total binding free energy (ΔG_bind). To confirm binding stability and thermodynamic favorability, the outcomes were contrasted with those of known inhibitors.

2.7 Thermal shift assay

Recombinant GST-tagged human CHEK1 protein was diluted in phosphate-buffered saline (PBS). Curcumin was dissolved in DMSO and incubated with the purified GST–CHEK1 protein or vehicle control at 37℃ for 30 min. The protein samples were then aliquoted and subjected to a temperature gradient of 37, 39, 41, 43, 45, 47, 49, 51, 53, and 55°C for 5 min at each temperature point. After heat treatment, samples were immediately cooled on ice and centrifuged to remove aggregated proteins. The soluble fractions were collected and analyzed by SDS–PAGE followed by Western blotting using an anti-GST antibody.

3 Results

3.1 Identification of Potential Targets of Curcumin in TNBC

The SwissTargetPrediction database provided a total of 65 potential curcumin targets. In the meantime, 6282 genes linked to TNBC were gathered from GeneCards. 58 overlapping targets were identified by the intersection of genes related to curcumin and TNBC; these targets were thought to be possible therapeutic targets of curcumin against TNBC (Fig. 1A). A compound–target–disease (C–T–D) network was built with Cytoscape in order to visualize the interactions between curcumin, its putative targets, and TNBC (Fig. 1B). Curcumin was shown as a blue node in this network, linked to 58 target proteins, which were then connected to the orange node, which stood for TNBC. The resulting network demonstrates the pharmacological activity of curcumin's multitarget and multi-pathway properties.

3.2 Functional Enrichment Analysis

Gene Ontology (GO) and Kyoto Encyclopedia of Genes and Genomes (KEGG) enrichment analyses were performed to better clarify the biological significance of the overlapping targets between curcumin and TNBC. To determine the main biological processes, cellular components, molecular functions, and signaling pathways involved in curcumin's pharmacological effects, 58 overlapping genes were examined (Fig. 2).

The targets were primarily enriched in processes associated with cellular response to nitrogen compound, cell cycle phase transition, inflammatory response, phosphorylation, and regulation of cellular response to stress in the biological process (BP) category (Fig. 2A). These results indicate that

curcumin may have anti-tumor effects through regulating inflammatory signaling, cell proliferation, and oxidative stress responses—biological processes that are often dysregulated in TNBC.

Significant enrichment was found for the cellular component (CC) category (Fig. 2B) in terms of focal adhesion, mitochondrial membrane, vesicle lumen, membrane raft, transcription regulator complex, and cyclin A2-CDK2 complex. According to these localizations, curcumin-targeted proteins primarily function in cytoplasmic and nuclear signal transduction, mitochondrial regulation, and cell adhesion—cellular processes essential for the growth and metastasis of tumors.

Phosphotransferase activity (alcohol group as acceptor), kinase binding, protein heterodimerization activity, MAP kinase activity, and cytokine binding were the primary enriched terms, according to the molecular function (MF) analysis (Fig. 2C). These findings demonstrate the critical role that protein–protein binding and kinase-related interactions play in curcumin's possible modulation of TNBC signaling networks.

Various cancer-associated pathways, such as the cell cycle (hsa04110), p53 signaling pathway (hsa04115), EGFR tyrosine kinase inhibitor resistance (hsa01521), HIF-1 signaling pathway (hsa04066), Apelin signaling pathway (hsa04371), and AGE-RAGE signaling pathway in diabetic complications (hsa04933), were significantly enriched in the KEGG pathway analysis (Fig. 2D). Furthermore, pathways like hormone signaling (hsa04081) and glucagon signaling (hsa04922) were also enriched, indicating that curcumin's action in TNBC may be influenced by metabolic and endocrine regulatory mechanisms.

When taken together, these enrichment results suggest that curcumin may modulate multiple pathways and targets to affect drug resistance, oxidative stress response, cell proliferation, and apoptosis in TNBC. This suggests a mechanistic basis for curcumin's possible therapeutic effects.

3.3 Protein–Protein Interaction (PPI) Network Construction

A PPI network was created in STRING using the 58 intersecting targets, and Cytoscape was used to visualize it (Fig. 3A). Curcumin-associated TNBC proteins were highly interconnected, as evidenced by the network's 58 nodes and 338 edges. Based on degree centrality, topological analysis identified a number of hub proteins, such as EGFR, AKT1, BCL2, and STAT3, suggesting that they play important roles in mediating the pharmacological activity of curcumin.

Additionally, each node's degree value was calculated and displayed as a bar chart to further illustrate the relative significance of each target in the network (Fig. 3B). The results demonstrated the crucial functions that AKT1, EGFR, STAT3, BCL2, AURKA, EP300, GSK3B, CDK2, CCNA2, CCNA1, CHEK1, BRAF, RPS6KB1 play in the curcumin–TNBC interaction network by displaying the lager than or equal to degree 10.

It's important to note that AURKA, CCNA2, CCNA1, CHEK1, BRAF, and RPS6KB1, have not been thoroughly examined in relation to TNBC or curcumin interaction. These results imply that curcumin

might have unknown regulatory effects on TNBC cell cycle and signaling regulation via these targets, which calls for additional verification using molecular docking and molecular dynamics simulation.

We examined the expression profiles of AURKA, CCNA2, CCNA1, CHEK1, BRAF, and RPS6KB1 in breast invasive carcinoma (BRCA) using the TCGA database in order to confirm the significance of these hub targets in breast cancer. Comparing BRCA tissues to normal controls, the results showed that CCNA1, BRAF, and RPS6KB1 were downregulated, while AURKA, CCNA2, and CHEK1 were significantly upregulated (Figure S1). These results offer more proof that these genes may be involved in the curcumin–TNBC network.

3.4 Molecular Docking Analysis

AURKA, CCNA2, CHEK1, and BRAF were chosen for molecular docking with curcumin based on the results of network analysis and differential expression in TNBC. Despite appearing as major nodes in the network as well, CCNA1 and RPS6KB1 were not included in the analysis as, according to a thorough literature review, there is currently no concrete evidence connecting them to TNBC. AURKA, CCNA2, CHEK1, and BRAF, on the other hand, have been shown to be biologically relevant targets for additional research due to their reported critical roles in tumor cell proliferation, DNA damage response, and oncogenic signaling.

To evaluate the binding affinity between curcumin and these four proteins, molecular docking was performed using AutoDock Vina. According to the docking results, curcumin exhibited stable binding to all of the targets. The binding energies were − 7.1 kcal/mol for CCNA2, − 6.8 kcal/mol for CHEK1, − 6.7 kcal/mol for AURKA, and − 6.5 kcal/mol for BRAF (Fig. 4A). The one with the lowest binding energy, CCNA2, indicated a stronger propensity to interact with curcumin.

Curcumin's special binding interactions with each protein were further demonstrated by visualizing the docking conformations.

Curcumin was found in a distinct hydrophobic pocket in CHEK1 (Fig. 4B), suggesting a common pocket-binding mode. Instead of being inside a distinct pocket, curcumin was found on the protein surface of CCNA2 (Fig. 4C), indicating a weaker or more surface-level interaction. Curcumin was evidently embedded in the binding pocket of AURKA, where it was held in place by numerous hydrogen bonds and hydrophobic contacts (Fig. 4D). Curcumin also filled a surface cavity in BRAF, which is in line with its capacity to alter kinase activity (Fig. 4E).

3.5 Molecular dynamics simulations of curcumin and target complexes

3.5.1 RMSD, RMSF, Rg analysis

CCNA2 was not included in MD simulations since curcumin was discovered to bind to the surface of CCNA2 instead of its active pocket. To investigate the dynamic stability and conformational changes of

the curcumin–protein complexes, 500 ns MD simulations were performed on the remaining three targets: AURKA, BRAF, and CHEK1. Nine systems were produced by simulating the apo forms of each protein and the corresponding positive inhibitors (Alisertib for AURKA, Vemurafenib for BRAF, and AZD7762 for CHEK1) for comparison (Bryant et al., 2014; Jalalirad et al., 2021; Pircher et al., 2021).

All simulated complexes achieved equilibrium in roughly 100–150 ns, as shown by the RMSD, RMSF, and Rg trajectories (Figure S2), and they all retained overall structural stability for the duration of the 500 ns simulation.

All three trajectories (apo, curcumin-bound, and alisertib-bound) for the AURKA systems (Figure S2A) stabilized during the simulation and reached equilibrium in about 100 ns. The curcumin–AURKA complex showed RMSD values of 0.25–0.35 nm, which were marginally lower than those of the apo form. This suggests that curcumin binding reduced large-scale conformational fluctuations and improved structural stability. Curcumin binding might stabilize AURKA similarly to its known inhibitor, according to the RMSD of the Alisertib complex, which showed a similar trend. After 150 ns, the RMSD values for the curcumin and Vemurafenib complexes in the BRAF systems (Figure S2B) stabilized at 0.3–0.4 nm, whereas the apo form showed somewhat greater fluctuations, peaking at 0.45 nm. In line with a clearly defined binding mode in the kinase pocket, this suggests that ligand binding, whether curcumin or vemurafenib, decreased backbone mobility and increased conformational rigidity. The RMSD trajectories of the curcumin- and AZD7762-bound systems for CHEK1 (Figure S2C) quickly converged (< 0.3 nm) and stayed steady for the full 500 ns. A slightly larger deviation (~ 0.35 nm) was seen in the apo system, indicating that curcumin binding encouraged a more stable and rigid protein conformation. Out of all the complexes, CHEK1–curcumin showed the smallest RMSD variations overall, indicating a particularly stable and tight binding.

A summary plot of the mean RMSD, RMSF, and Rg values was created in order to compare the overall stability of all systems in more detail (Figure S2D). The results demonstrated that, while retaining comparable compactness (Rg), curcumin-bound systems showed consistently lower RMSD and RMSF values than apo and inhibitor-bound complexes. Its superior dynamic stability was confirmed by the fact that CHEK1-curcumin showed the lowest RMSD of all.

According to RMSF values, in all systems, residues in the enzyme and binding domains stayed mostly rigid, while the largest fluctuations took place in the terminal or loop regions.

Curcumin binding may constrain these motifs similarly to Alisertib, as evidenced by the slight flexibility differences between the curcumin- and inhibitor-bound systems of AURKA's αC-helix and activation loop, which are important regulatory regions in kinase activity.

In BRAF, loop segments distant from the active site were represented by modest peaks in RMSF between residues 550 and 620. In contrast to the apo form, curcumin binding reduced these motions, which further suggests stabilizing effects on the protein core.

All systems showed almost constant Rg values over time, with AURKA (~ 1.9 nm), BRAF (~ 1.95 nm), and CHEK1 (~ 1.9–2.0 nm). The Rg is a measure of the global compactness of the protein structure. Interestingly, Rg was generally slightly lower in ligand-bound complexes than in apo forms, suggesting a more compact structure upon ligand association.

The fact that Rg varied only slightly (< 0.05 nm) over all trajectories indicates that there was no substantial unfolding or structural expansion, indicating that all systems were well-equilibrated and conformationally stable throughout the simulation.

While taken together, RMSD, RMSF, and Rg analyses show that curcumin formed compact and stable complexes with AURKA, BRAF, and CHEK1 that were on level with or even marginally more stable than those of their respective positive inhibitors. These results suggest that curcumin not only binds to these kinases' functional pockets but also provides conformational stability, which may be the basis for its ability to inhibit signaling pathways linked to TNBC.

3.5.2 FEL Analysis

The first two principal components (PC1 and PC2) obtained from PCA were used to build the FEL in order to further investigate the conformational stability and energy states of each system (Figure S3).

In the absence of a ligand, the Apo system for AURKA (Figure S3A) displayed a comparatively wide and distributed energy basin, suggesting high conformational flexibility. The energy surfaces showed a single dominant deep basin upon binding with either Curcumin (Figure S3B) or the positive control Alisertib (Figure S3C), indicating that ligand binding stabilized the protein structure and constrained the conformational space. Interestingly, the energy depth of the Curcumin–AURKA complex was comparable to that of the Alisertib–AURKA complex, suggesting similar conformational stability. The Apo form (Figure S3D) in the BRAF systems showed several shallow minima, which were indicative of structural fluctuations throughout the simulation. One noticeable deep minimum was seen in the Curcumin-BRAF complex (Figure S3E), suggesting that Curcumin binding maintained a particular conformational state. Although slightly wider than Curcumin's, the Vemurafenib–BRAF complex (Figure S3F) also showed a deep single basin, indicating that Curcumin induces a more compact conformational ensemble than the known inhibitor. Higher flexibility was indicated by the Apo form's (Figure S3G) distributed and less defined energy surface for CHEK1. On the other hand, the AZD7762–CHEK1 (Figure S3I) and Curcumin–CHEK1 (Figure S3H) complexes, showed a single narrow and deep energy basin, suggesting increased structural rigidity and stability upon ligand binding.

Curcumin binding decreases conformational heterogeneity and improves the structural stability of AURKA, BRAF, and CHEK1, just like their respective positive control inhibitors, according to the FEL results, which were in agreement with RMSD, RMSF, and Rg analyses.

3.6 Binding Free Energy Analysis

100 snapshots evenly extracted from the 100 ns with lowest FEL of each trajectory were used for MM/PBSA calculations to further measure Curcumin's binding affinities with the chosen target proteins. Figure 5 displays the determined binding free energies (ΔG_binding) for the Curcumin–target complexes and the positive controls that correspond to them.

The thermodynamically favorable binding was confirmed by the negative ΔG_binding values displayed by all complexes. The curcumin–target systems with the best affinities were CHEK1 (–209.37 kJ/mol) and BRAF (–192.87 kJ/mol), whereas AURKA (–135.64 kJ/mol) had a moderate binding energy. Curcumin may interact with these kinases in a functionally relevant way, as evidenced by the fact that its ΔG_binding toward BRAF and CHEK1 was similar to that of the clinically validated inhibitors Vemurafenib (–247.23 kJ/mol) and AZD7762 (–177.12 kJ/mol), respectively. In accordance with the hydrophobic and hydrogen-bonding properties of the ligand–protein interfaces, the decomposition of energy components revealed that van der Waals (ΔG_vdw) and electrostatic (COU) interactions were the main contributors to binding stability. Together with the MD and FEL analyses, these results provide compelling evidence for AURKA, BRAF, and CHEK1 as putative binding sites via which curcumin may have anti-TNBC effects.

3.7 Binding mode analysis of Curcumin and reference inhibitors with CHEK1, BRAF, and AURKA

The representative lowest-energy conformations from the FEL landscapes were chosen out, and interaction analyses were carried out for every protein–ligand complex in order to better clarify the molecular interactions between Curcumin and its main target proteins (Fig. 6).

Curcumin formed numerous hydrogen bonds and hydrophobic contacts with residues like Leu15, Val23, Lys38, Leu84, Cys87 and Leu137 in the CHEK1–Curcumin complex (Fig. 6A), indicating a strong binding affinity and possible inhibitory activity. Curcumin was stably located within the catalytic pocket of CHEK1. The docking site's dependability was confirmed by the reference inhibitor AZD7762 (Fig. 6B), which likewise bound deeply within the same pocket and interacted with Leu15, Val23, Ala36, Leu84, Cys87, Leu137 and Asp148. Curcumin occupied the ATP-binding pocket in the BRAF–Curcumin complex (Fig. 6C), through hydrogen bonding and π–π interactions with residues Ile463, Leu505, Leu514, Trp531, Phe583 and Asp594. In line with its established inhibitory mechanism against BRAF, the FDA-approved inhibitor Vemurafenib (Fig. 6D) bound to a similar region through hydrogen bonding and π–π interactions with residues Phe468, Val471, Ala481, Trp531, Cys532 and Phe595. Similarly, Curcumin formed stable interactions with residues Leu139, Ala160, Ala213, Arg220 and Leu263 after embedding itself in the active pocket of AURKA (Fig. 6E). The dependability of the docking results was confirmed by the control compound Alisertib (Fig. 6F), which displayed similar binding localization and interaction patterns, including hydrogen bonds and hydrophobic interactions with Lys143, Phe144, Phe165, Gln168, Ala172 and Val174.

3.8 Curcumin can bind to CHEK1

Purified GST-tagged CHEK1 protein was used in an in vitro cellular thermal shift-like assay to confirm the computational prediction that CHEK1 is a novel molecular target of curcumin. Protein thermal shift was evaluated by immunoblot (IB) analysis after the protein was incubated with or without curcumin (20 μM) and exposed to a temperature gradient between 37°C and 55°C (Fig. 7). GST-CHEK1 showed a significant temperature-dependent decrease in soluble protein levels in the absence of curcumin (DMSO control), with a sharp decrease noted at temperatures above 45°C, indicating progressive thermal denaturation. Curcumin-treated samples, on the other hand, demonstrated significantly improved thermal stability over the same temperature range, retaining a significantly larger percentage of soluble CHEK1 at higher temperatures.

Together, these results demonstrate that curcumin directly interacts with CHEK1 and increases its thermal stability in vitro, providing experimental evidence to support CHEK1 as a bona fide target of curcumin.

4 Discussion

Since it lacks the ER, PR, and HER2, TNBC is one of the most aggressive and difficult to treat subtypes of breast cancer. Chemotherapy is the primary treatment option due to the lack of clearly defined molecular targets. However, it has severe toxicity and limited efficacy. As a result, identifying novel molecular targets and therapeutic agents for TNBC is crucial. Due to their multifaceted mechanisms and low toxicity, plant compounds have garnered a lot of attention recently as promising anticancer candidates. One of among them, curcumin, a naturally occurring polyphenolic compound that comes from Curcuma longa L. and has shown promising anticancer properties against a number of cancers, including TNBC. However, its exact molecular targets and mechanisms in TNBC are still unknown. To address this therapeutic gap and identify new potential mechanisms of curcumin in TNBC treatment, the current study used an integrated computational approach to methodically investigate curcumin's potential molecular targets and mechanisms in TNBC with the objective.

An integrated network pharmacology and molecular simulation approach was used in this study to identify curcumin's possible targets and mechanisms of action against TNBC. Potential curcumin-interacting targets that are biologically and clinically significant include AURKA, BRAF, and CHEK1. The hallmark processes that propel TNBC proliferation, metastasis, and treatment resistance are cell cycle progression, DNA damage response, and oncogenic signaling, all of which are significantly regulated by these kinases (Jalalirad et al., 2021; Li et al., 2023; B. Wang et al., 2024; S. H. Wang et al., 2024).

The progression of TNBC, resistance to treatment, and poor prognosis are all largely caused by AURKA (Jalalirad et al., 2021). When compared to normal and luminal breast cancer subtypes, it is consistently overexpressed in TNBC, which is associated with higher rates of proliferation and poorer survival outcomes (Sun et al., 2021). Mechanistically, AURKA supports chemoresistance, cancer stem cell maintenance, and epithelial–mesenchymal transition (EMT), especially after taxane-based chemotherapy (Jalalirad et al., 2021; Ning et al., 2025; Sun et al., 2021). AURKA's nuclear localization

promotes PD-L1 expression, which makes immune evasion easier (Takchi et al., 2024). It has been demonstrated that use AURKA inhibitors, such as alisertib, can inhibit tumor growth, decreases stemness, and increases immune cell infiltration (Takchi et al., 2024). Additionally, in preclinical TNBC models, combination strategies like AURKA–PD-L1 blockade or AURKA–CHEK1 dual inhibition produce synergistic antitumor effects (Pellizzari et al., 2024).

BRAF, a serine/threonine kinase in the RAS–RAF–MEK–ERK cascade, is another key player in cellular survival and proliferation (Degirmenci et al., 2020). Even though TNBC rarely has BRAF mutations, the V600E variant is a tiny but potentially useful subset (Shi et al., 2018). Targeted BRAF inhibition may be beneficial in certain situations, as evidenced by clinical reports of TNBC patients with BRAF(V600E) mutations who experienced partial or prolonged responses to vemurafenib or dabrafenib treatment (Ku et al., 2022; Pircher et al., 2021). Moreover, TNBC aggression is influenced by abnormal MAPK pathway activation even when there is no direct BRAF mutation (Shi et al., 2018). The BRAF(V600E) mutant receptor was used in this study's molecular docking and MD simulations, which offered structural insights into curcumin's potential modulation of this oncogenic kinase.

Molecular docking analysis was carried out for AURKA, BRAF, and CHEK1 in order to investigate curcumin's binding potential toward the identified kinase targets in more detail. With docking scores of − 6.7 kcal/mol for AURKA, − 6.5 kcal/mol for BRAF, and − 6.8 kcal/mol for CHEK1, curcumin demonstrated favorable binding affinities. These values were either similar to or marginally lower than those of their respective reference inhibitors, AZD7762 (–6.7 kcal/mol), Vemurafenib (–9.7 kcal/mol), and Alisertib (–8.7 kcal/mol). Curcumin forms numerous hydrogen bonds and hydrophobic interactions in the ATP-binding cleft or catalytic pocket of these kinases, according to structural visualization. Curcumin may interfere with ATP binding to produce competitive inhibitory effects, as suggested by its overlapping position and known inhibitors.

Alisertib has demonstrated strong anti-TNBC effects by inhibiting the epithelial-to-mesenchymal transition (EMT), decreasing the number of cancer stem-like cells (CSCs), and lowering the expression of PD-L1, which increases the infiltration of CD8 + T cells and their sensitivity to chemotherapy (Skov et al., 2022; Takchi & Haddad, 2023). By interfering with the AURKA–AKT and TGF-β signaling pathways, it also prevents metastasis and reverses chemoresistance (Jalalirad et al., 2021). Curcumin binds within the same ATP pocket that alisertib targets, according to the docking results. This suggests that curcumin may mimic AURKA inhibition and thereby suppress mitotic progression and proliferation in TNBC.

BRAF V600E, account for about 2–3% of triple-negative breast cancers, activates the constitutive MAPK pathway to promote tumor growth. According to available data, BRAF V600E might function as a predictive biomarker for the response to targeted therapy (Ku et al., 2022; L. Y. Wang et al., 2022). Vemurafenib, a selective BRAF V600E inhibitor, has been shown in clinical case reports to produce both radiological and clinical responses in metastatic TNBC that carries this mutation (Pircher et al., 2021). Preclinical research also demonstrates that BRAF-mutant TNBC cell lines exhibit apoptosis and cell cycle arrest in response to treatment, demonstrating their high sensitivity to BRAF and MEK inhibition

(Ku et al., 2022; L. Y. Wang et al., 2022). According to this study, curcumin may disrupt MAPK signaling because it bound to the catalytic pocket of BRAF for ATP coordination and kinase activation (Deng et al., 2022). This is in line with earlier research showing curcumin inhibits TNBC cell proliferation and suppresses ERK phosphorylation, indicating the possibility of modifying MAPK-driven tumor progression even in wild-type BRAF settings (Chen et al., 2024). In TNBC models, the ATP-competitive CHEK1 inhibitor AZD7762 has demonstrated strong synergistic effects with radiotherapy and DNA-damaging agents (such as carboplatin, irinotecan, and gemcitabine), causing mitotic catastrophe, multinucleation, and apoptosis (Ma et al., 2012; Zhu et al., 2021). Additionally, it increases the effectiveness of PARP or AURKA inhibitors, providing justification for combination treatment plans in resistant TNBC (Li et al., 2023). Curcumin showed consistent docking in the ATP-binding site of CHEK1 in this investigation, which overlapped with the binding region of AZD7762. This implies that curcumin may disrupt CHEK1-mediated checkpoint signaling, which could cause TNBC cells to accumulate DNA damage and undergo apoptosis.

Thorough MD simulations have been performed out over 500 ns for each curcumin–protein complex, along with their corresponding apo forms and reference inhibitor-bound systems, in order to get a deeper comprehension of the dynamic stability and conformational effects of curcumin binding to the identified protein targets. These complexes' dynamic behavior provides important insights into binding stability and possible atomic-level inhibitory mechanisms. All of the simulated curcumin–protein complexes reached equilibrium after around 50 ns, according to the RMSD trajectories, with stable fluctuations within 0.2–0.3 nm, indicating well-converged and energetically stable systems. Curcumin forms stable and long-lasting interactions with the active sites of these kinases, as evidenced by the fact that the RMSD values of the curcumin–CHEK1 and curcumin–BRAF complexes were similar to or even slightly lower than those of the positive control complexes (AZD7762–CHEK1 and Vemurafenib–BRAF). Strong binding affinities and effective conformational adaptation of the ligand to the protein pocket are frequently linked to such stability. According to additional analysis of residue flexibility through RMSF calculation, Curcumin binding significantly decreased fluctuations in pocket regions, especially within the ATP-binding splits of CHEK1 and BRAF. Curcumin could limit local conformational motions necessary for catalytic renewal, as evidenced by the significantly reduced flexibility of CHEK1 residues surrounding the catalytic domain (particularly around the hinge and activation loop) when compared to the apo protein. The kinase domain's rigidity could hinder the conformational modifications necessary for substrate binding and phosphorylation, which would reduce enzymatic activity. Further evidence of conformational stabilization and inhibition of active-state dynamics was provided by the reduced fluctuations in the activation segment. In addition to the RMSD and RMSF results, the Rg analysis revealed that the curcumin–protein complexes had slightly lower Rg values than their free counterparts, indicating a more compact secondary structure. According to the hypothesis that curcumin aids in structural stabilization by forming numerous hydrophilic interactions and hydrogen-bonding interactions within the binding pocket, this compaction is indicative of stronger internal packing and improved structural integrity upon ligand binding.

FEL analysis revealed more details about the systems' conformational energetics. More details about the systems' conformational energetics were revealed by FEL analysis. The curcumin-bound proteins' FEL graphs displayed deep, narrow energy basins that matched a single dominant conformational position with few substate shifts. On the other hand, the apo systems exhibited shallower and wider basin landscapes, which is a sign of dynamic variability and higher conformational energy. The CHEK1–curcumin system displayed the most compact and lowest-energy basin among the complexes that were examined, indicating a highly stable and energetically advantageous conformation. The effect observed in the AZD7762–CHEK1 complex is similar to this energetic confinement, indicating that curcumin binding also stabilizes CHEK1 in a catalytically inactive conformation.

MM/PBSA free energy calculations have been conducted using the lowest-energy 100 frames from each FEL in order to quantitatively validate these observations. Curcumin's ΔG_binding values were − 135.64 kJ/mol (AURKA), − 192.87 kJ/mol (BRAF), and − 209.37 kJ/mol (CHEK1), indicating strong binding affinities toward all three kinases. Stronger binding stability was indicated by CHEK1–curcumin's substantially lower total binding energy when compared to AZD7762 (–177.12 kJ/mol). Curcumin's affinity for AURKA was within the same energetic range as Alisertib (–195.81 kJ/mol), and its binding energy to BRAF was similar to that of Vemurafenib (–247.23 kJ/mol). According to hydrophobic binding patterns typically observed for curcumin and kinase inhibitors, the decomposition of energy terms showed that van der Waals and electrostatic interactions were the main forces behind binding, while the polar solvation term had an adverse contribution.

Curcumin's strong binding within the hydrophobic core of CHEK1 was further confirmed by structural interaction analysis of the most stable conformations. It forms hydrophobic interactions with Leu137 and Ile37 and hydrogen bonds with Leu15, Cys87, and Val23. The hypothesis that curcumin may inhibit CHEK1 by blocking the ATP-binding site is supported by the 2D interaction maps, which indicated that the binding pocket residues largely overlap with those of AZD7762. Similar to the Vemurafenib-binding mode, the BRAF–curcumin complex's ligand was stabilized in the hinge region of the kinase domain by the interaction with Asp594 and Phe583 via π–π stacking and hydrogen bonding. Curcumin demonstrated a common mechanism of inhibition for AURKA by forming stable hydrophobic contacts with Leu139, Ala160, and Leu263, which have been demonstrated to stabilize Alisertib.

Each of these structural and energetic evaluations indicate CHEK1 as possibly the most promising target for curcumin therapy in TNBC. Curcumin may act as a potential natural CHEK1 inhibitor, interfering with checkpoint signaling and causing cell cycle arrest, according to the study's findings on the CHEK1–curcumin complex's superior binding energy and conformational stability. This is consistent with earlier experimental results showing (Almalki et al., 2023).

In summary, curcumin exhibits anti-TNBC activity through a multitarget mechanism involving AURKA, BRAF, and CHEK1, according to our integrated computational analyses. The current study identifies CHEK1 as a previously unidentified target as a possible binding receptor of curcumin, in contrast to earlier network pharmacology reports on curcumin in TNBC that focused mainly on classical pathways

like PI3K/Akt, MAPK, JAK/STAT, or Wnt/β-catenin signaling (Chen et al., 2024; Deng et al., 2022). As far as we are aware, this is the first integrated computational study to show that curcumin may interact directly with CHEK1 at a binding free energy similar to that of the inhibitor AZD7762, which has been clinically validated. This discovery offers a fresh mechanistic explanation for curcumin's anti-TNBC action by interfering with the DNA damage checkpoint pathway, which has not been clarified in previous studies. Curcumin could act as a natural checkpoint suppressor, causing cancer cells more sensitive to genetic stress by limiting the conformational dynamics of CHEK1 and maintaining an inactive-like state. This mechanism is consistent with the evidence that TNBC sensitivity to radiation and chemotherapy can be effectively increased by dual inhibition of cell cycle checkpoints and DNA repair. Thermal stability assays are widely used to assess direct ligand–protein interactions based on the principle that ligand binding often stabilizes the native conformation of a protein, thereby increasing its resistance to thermal denaturation. In our assay, curcumin treatment resulted in a clear stabilization of GST-tagged CHEK1, as reflected by the increased soluble protein fraction at elevated temperatures. This thermal protection effect strongly suggests direct binding of curcumin to CHEK1 rather than an indirect or nonspecific interaction. Furthermore, the current work used the oncogenic BRAF(V600E) mutant structure, which accounts for about 2–3% of TNBC cases, in contrast to the majority of previous studies that used wild-type BRAF for docking and pathway analysis. According to this mutation-specific analysis, Curcumin can occupy the same ATP-binding pocket as vemurafenib, which suggests a potential interaction mode pertinent to this clinically actionable subset of TNBC. This study methodologically expands on earlier curcumin–TNBC investigations by providing dynamic and thermodynamic validation of ligand–protein stability beyond static docking predictions by using FEL analyses and long-timescale (500 ns) molecular dynamics simulations. These differences all contribute to constitute a thorough and mechanistically refined investigation of curcumin's multitarget potential against TNBC in the current work.

Further lead optimization and structural modification will be investigated in considering native curcumin's drawbacks, such as poor solubility, low systemic stability, and rapid metabolism. Target affinity, bioavailability, and metabolic stability may all be enhanced by the development of curcumin derivatives with optimized substituents. Finding effective curcumin-based kinase inhibitors will be accelerated up even more with computational modeling and experimental validation of synthetic analogs. The thermal shift assay was performed using purified protein in vitro, which does not fully recapitulate the cellular environment. Future studies using cellular CETSA, enzymatic activity assays, or mutational analysis of the predicted binding site will be necessary to further confirm the functional relevance of the curcumin–CHEK1 interaction in cells.

Furthermore, the complete experimental validation process will be guided by these computational results. In future, initially, in vitro experiments, such as IC_{50} determination, cell proliferation and colony formation assays, and DNA damage analysis, will warrant to confirm curcumin's inhibitory effects. In particular, these investigations will shed light on curcumin's effects on checkpoint signaling and apoptosis induction, as well as its dose-dependent cytotoxic profile and mechanistic effects on TNBC cell lines. Curcumin's antitumor efficacy, pharmacokinetics, and biosafety will then be evaluated in vivo xenograft experiments in mice, offering vital preclinical evidence for translational potential.

Taken together, this study is an outstanding instance of how network pharmacology and dynamic simulations can be used to clarify the multi-target mechanisms of natural products. And these findings clarify the molecular mechanism of curcumin's multitarget inhibitory action against TNBC, and they also provide an accurate theoretical and methodological basis for the compound's future development as a natural lead. Curcumin and its analogs may eventually progress toward clinically effective treatments for TNBC through the future integration of computational modeling, medicinal chemistry, and biological validation.

5 Conclusions

AURKA, BRAF, and CHEK1 have been identified to be significant curcumin-binding targets in TNBC. Stable and advantageous interactions have been discovered using molecular docking and dynamics analyses, with CHEK1 exhibiting the highest affinity. These results imply that curcumin inhibits multiple targets via DNA damage, MAPK, and mitotic pathways. Furthermore, structural optimization may produce more potent derivatives for TNBC therapy, and curcumin may be a promising lead compound.

6 Limitation

Meanwhile, this study also has several limitations. First, the analysis was based on publicly available databases and computer simulations, and the size of the dataset depended on the coverage and quality of the selected databases. Second, although network pharmacology, molecular docking, and molecular dynamics simulations suggested potential curcumin binding targets in triple-negative breast cancer, most findings were derived from computer predictions. Besides the thermal displacement experiment confirming the interaction between curcumin and CHEK1, further experimental validation, including cellular and in vivo functional experiments, is needed. Therefore, this study provides a mechanistic and hypothesis-generating framework worthy of further biological and clinical investigation.

Abbreviations

AKT: Protein Kinase B

AR: Androgen Receptor

BH: Benjamini–Hochberg

BP: Biological Process

BRCA: Breast Invasive Carcinoma

CC: Cellular Component

C–T–D: Compound–Target–Disease

EGFR: Epidermal Growth Factor Receptor

EMT: Epithelial–Mesenchymal Transition

FEL: Free Energy Landscape

GO: Gene Ontology

KEGG: Kyoto Encyclopedia of Genes and Genomes

mTOR: Mechanistic/Mammalian Target of Rapamycin

MM-PBSA: Molecular Mechanics Poisson–Boltzmann Surface Area

PCA: Principal Component Analysis

PI3K: Phosphoinositide 3-Kinase

PPI: Protein–Protein Interaction

Rg: Radius of Gyration

RMSD: Root Mean Square Deviation

RMSF: Root Mean Square Fluctuation

TNBC: Triple-Negative Breast Cancer

PBS: Phosphate-buffered Saline

IB: Immunoblotting

Declarations

Ethics approval and consent to participate

Not applicable.

Consent for publication

Not applicable.

Availability of data and materials

Curcumin-related targets were predicted using the SwissTargetPrediction database (https://www.swisstargetprediction.ch/). Triple-negative breast cancer (TNBC)-associated genes were collected from the GeneCards database (https://www.genecards.org/). Protein–protein interaction (PPI) networks were constructed using the STRING database v12.0 (https://string-db.org/). Gene Ontology (GO) and Kyoto Encyclopedia of Genes and Genomes (KEGG) pathway enrichment analyses were performed using Metascape (https://metascape.org/). Protein structures of AURKA (PDB ID: 5L8L), BRAF V600E (PDB ID: 8C7Y), and CHEK1 (PDB ID: 2YEX) were obtained from the RCSB Protein Data Bank

(https://www.rcsb.org/). The three-dimensional structure of curcumin was downloaded from PubChem (CID: 969516) (https://pubchem.ncbi.nlm.nih.gov/). All other data supporting the findings of this study are available from the corresponding author upon reasonable request..

Competing interests

The authors declare no competing interests.

Funding

This research did not receive any specific grant from funding agencies in the public, commercial, or not-for-profit sectors.

Authors' contributions

XQ and YW designed the study. XQ, HZ, and LQ performed the investigation, validation, and data curation. SW and LM developed the software and visualizations. XQ conducted the formal analysis and wrote the original draft. The work was supervised and administered by KZ and YW, who also oversaw the manuscript reviewing and editing with input from all authors. All authors declare that all data were generated in-house, that no paper mill was used and that no AI tool has been used for the generation of text or figures.

Acknowledgements

Not applicable.

References

1. Almalki, E., Al-Amri, A., Alrashed, R., AL-Zharani, M., & Semlali, A. (2023). The Curcumin Analog PAC Is a Potential Solution for the Treatment of Triple-Negative Breast Cancer by Modulating the Gene

Expression of DNA Repair Pathways. *International Journal of Molecular Sciences*, *24*(11). https://doi.org/ARTN 964910.3390/ijms24119649

2. Bryant, C., Rawlinson, R., & Massey, A. J. (2014). Chk1 Inhibition as a novel therapeutic strategy for treating triple-negative breast and ovarian cancers. *Bmc Cancer*, *14*. https://doi.org/Artn 57010.1186/1471-2407-14-570
3. Chen, Z., Lu, P. J., Li, M. H., Zhang, Q., He, T., & Gan, L. (2024). Curcumin suppresses metastasis of triple-negative breast cancer cells by modulating EMT signaling pathways: An integrated study of bioinformatics analysis. *Medicine*, *103*(8). https://doi.org/ARTN e3726410.1097/MD.0000000000037264
4. Cheng, T. C., Sayseng, J. O., Tu, S. H., Juan, T. C., Fang, C. L., Liao, Y. C., Chu, C. Y., Chang, H. W., Yen, Y., Chen, L. C., & Ho, Y. S. (2021). Curcumin-induced antitumor effects on triple-negative breast cancer patient-derived xenograft tumor mice through inhibiting salt-induced kinase-3 protein. *Journal of Food and Drug Analysis*, *29*(4), 622-637. https://doi.org/10.38212/2224-6614.3387
5. Daina, A., Michielin, O., & Zoete, V. (2019). SwissTargetPrediction: updated data and new features for efficient prediction of protein targets of small molecules. *Nucleic Acids Res*, *47*(W1), W357-W364. https://doi.org/10.1093/nar/gkz382
6. Degirmenci, U., Wang, M., & Hu, J. C. (2020). Targeting Aberrant RAS/RAF/MEK/ERK Signaling for Cancer Therapy. *Cells*, *9*(1). https://doi.org/ARTN 19810.3390/cells9010198
7. Deng, Z. C., Chen, G. H., Shi, Y. H., Lin, Y., Ou, J. B., Zhu, H., Wu, J. Y., Li, G. C., & Lv, L. (2022). Curcumin and its nano-formulations: Defining triple-negative breast cancer targets through network pharmacology, molecular docking, and experimental verification. *Frontiers in Pharmacology*, *13*. https://doi.org/ARTN 92051410.3389/fphar.2022.920514
8. Dong, S. L., & Alahari, S. K. (2020). Combination treatment of bicalutamide and curcumin has a strong therapeutic effect on androgen receptor-positive triple-negative breast cancers. *Anti-Cancer Drugs*, *31*(4), 359-367. https://doi.org/10.1097/Cad.0000000000000880
9. Farghadani, R., & Naidu, R. (2021). Curcumin: Modulator of Key Molecular Signaling Pathways in Hormone-Independent Breast Cancer. *Cancers*, *13*(14). https://doi.org/ARTN 342710.3390/cancers13143427
10. Forli, S., Huey, R., Pique, M. E., Sanner, M. F., Goodsell, D. S., & Olson, A. J. (2016). Computational protein-ligand docking and virtual drug screening with the AutoDock suite. *Nature Protocols*, *11*(5), 905-919. https://doi.org/10.1038/nprot.2016.051
11. Gupta, G. K., Collier, A. L., Lee, D., Hoefer, R. A., Zheleva, V., van Reesema, L. S. L., Tang-Tan, A. M., Guye, M. L., Chang, D. Z., Winston, J. S., Samli, B., Jansen, R. J., Petricoin, E. F., Goetz, M. P., Bear, H. D., & Tang, A. H. (2020). Perspectives on Triple-Negative Breast Cancer: Current Treatment Strategies, Unmet Needs, and Potential Targets for Future Therapies. *Cancers*, *12*(9). https://doi.org/ARTN 239210.3390/cancers12092392
12. Guterres, H., & Im, W. (2020). Improving Protein-Ligand Docking Results with High-Throughput Molecular Dynamics Simulations. *J Chem Inf Model*, *60*(4), 2189-2198.

https://doi.org/10.1021/acs.jcim.0c00057

13. Hashem, S., Ali, T. A., Akhtar, S., Nisar, S., Sageena, G., Ali, S., Al-Mannai, S., Therachiyil, L., Mir, R., Elfaki, I., Mir, M. M., Jamal, F., Masoodi, T., Uddin, S., Singh, M., Haris, M., Macha, M., & Bhat, A. A. (2022). Targeting cancer signaling pathways by natural products: Exploring promising anti-cancer agents. *Biomedicine & Pharmacotherapy*, *150*. https://doi.org/ARTN 11305410.1016/j.biopha.2022.113054
14. Howard, F. M., & Olopade, O. (2021). Epidemiology of Triple-Negative Breast Cancer A Review. *Cancer Journal*, *27*(1), 8-16. https://doi.org/10.1097/Ppo.0000000000000500
15. Iwasa, J., Goodsell, D. S., Burley, S. K., & Zardecki, C. (2025). A new chapter for RCSB Protein Data Bank Molecule of the Month in 2025. *Structural Dynamics-Us*, *12*(2). https://doi.org/Artn 02110110.1063/4.0000302
16. Jalalirad, M., Haddad, T. C., Salisbury, J. L., Radisky, D., Zhang, M. Z., Schroeder, M., Tuma, A., Leof, E., Carter, J. M., Degnim, A. C., Boughey, J. C., Sarkaria, J., Yu, J., Wang, L. W., Liu, M. C., Zammataro, L., Malatino, L., Galanis, E., Ingle, J. N., . . . D'Assoro, A. B. (2021). Aurora-A kinase oncogenic signaling mediates TGF-β-induced triple-negative breast cancer plasticity and chemoresistance. *Oncogene*, *40*(14), 2509-2523. https://doi.org/10.1038/s41388-021-01711-x
17. Kocaadam, B., & Sanlier, N. (2017). Curcumin, an active component of turmeric (Curcuma longa), and its effects on health. *Critical Reviews in Food Science and Nutrition*, *57*(13), 2889-2895. https://doi.org/10.1080/10408398.2015.1077195
18. Ku, G. C., Chapdelaine, A. G., Ayrapetov, M. K., & Sun, G. Q. (2022). Identification of Lethal Inhibitors and Inhibitor Combinations for Mono-Driver versus Multi-Driver Triple-Negative Breast Cancer Cells. *Cancers*, *14*(16). https://doi.org/ARTN 402710.3390/cancers14164027
19. Kumari, R., Kumar, R., Lynn, A., & Consort, O. S. D. D. (2014). A GROMACS Tool for High-Throughput MM-PBSA Calculations. *Journal of Chemical Information and Modeling*, *54*(7), 1951-1962. https://doi.org/10.1021/ci500020m
20. Lashkov, A. A., Tolmachev, I. V., Eistrikh-Heller, P. A., & Rubinsky, S. V. (2021). PyFepRestr: Plugin to PyMOL Molecular Graphics System for Calculating the Free Energy of Ligand-Receptor Binding. *Crystallography Reports*, *66*(5), 861-865. https://doi.org/10.1134/S1063774521050126
21. Li, C. Y., Liao, J. T., Wang, X. Y., Chen, F. X., Guo, X. M., & Chen, X. X. (2023). Combined Aurora Kinase A and CHK1 Inhibition Enhances Radiosensitivity of Triple-Negative Breast Cancer Through Induction of Apoptosis and Mitotic Catastrophe Associated With Excessive DNA Damage. *International Journal of Radiation Oncology Biology Physics*, *117*(5), 1241-1254. https://doi.org/10.1016/j.ijrobp.2023.06.022
22. Li, M. J., Guo, T. T., Lin, J. Y., Huang, X., Ke, Q. D., Wu, Y. J., Fang, C. P., & Hu, C. X. (2022). Curcumin inhibits the invasion and metastasis of triple negative breast cancer via Hedgehog/Gli1 signaling pathway. *Journal of Ethnopharmacology*, *283*. https://doi.org/ARTN 11468910.1016/j.jep.2021.114689

23. Li, Y., Zhan, Z. J., Yin, X. M., Fu, S. J., & Deng, X. Y. (2021). Targeted Therapeutic Strategies for Triple-Negative Breast Cancer. *Frontiers in Oncology*, *11*. https://doi.org/ARTN 73153510.3389/fonc.2021.731535
24. Liu, L., Fu, Y. L., Zheng, Y. Y., Ma, M. K., & Wang, C. H. (2020). Curcumin inhibits proteasome activity in triple-negative breast cancer cells through regulating p300/miR-142-3p/PSMB5 axis. *Phytomedicine*, *78*. https://doi.org/ARTN 15331210.1016/j.phymed.2020.153312
25. Ma, C. X., Cai, S. R., Li, S. Q., Ryan, C. E., Guo, Z. F., Schaiff, W. T., Lin, L., Hoog, J., Goiffon, R. J., Prat, A., Aft, R. L., Ellis, M. J., & Piwnica-Worms, H. (2012). Targeting Chk1 in p53-deficient triple-negative breast cancer is therapeutically beneficial in human-in-mouse tumor models. *Journal of Clinical Investigation*, *122*(4), 1541-1552. https://doi.org/10.1172/Jci58765
26. Naeem, A., Hu, P. Y., Yang, M., Zhang, J., Liu, Y. L., Zhu, W. F., & Zheng, Q. (2022). Natural Products as Anticancer Agents: Current Status and Future Perspectives. *Molecules*, *27*(23). https://doi.org/ARTN 836710.3390/molecules27238367
27. Ning, B. H., Liu, C., Kucukdagli, A. C., Zhang, J. Y., Jing, H., Zhou, Z. Q., Zhang, Y. W., Dong, Y., Chen, Y. J., Guo, H., & Xu, J. (2025). Proteomic profiling identifies upregulation of aurora kinases causing resistance to taxane-type chemotherapy in triple negative breast cancer. *Scientific Reports*, *15*(1). https://doi.org/ARTN 321110.1038/s41598-025-87315-x
28. Noor, F., Tahir Ul Qamar, M., Ashfaq, U. A., Albutti, A., Alwashmi, A. S. S., & Aljasir, M. A. (2022). Network Pharmacology Approach for Medicinal Plants: Review and Assessment. *Pharmaceuticals (Basel)*, *15*(5). https://doi.org/10.3390/ph15050572
29. Obidiro, O., Battogtokh, G., & Akala, E. O. (2023). Triple Negative Breast Cancer Treatment Options and Limitations: Future Outlook. *Pharmaceutics*, *15*(7). https://doi.org/ARTN 179610.3390/pharmaceutics15071796
30. Pellizzari, S., Athwal, H., Bonvissuto, A. C., & Parsyan, A. (2024). Role of AURKB Inhibition in Reducing Proliferation and Enhancing Effects of Radiotherapy in Triple-Negative Breast Cancer. *Breast Cancer-Targets and Therapy*, *16*, 341-346. https://doi.org/10.2147/Bctt.S444965
31. Pircher, M., Winder, T., & Trojan, A. (2021). Response to Vemurafenib in Metastatic Triple-Negative Breast Cancer Harbouring a BRAF V600E Mutation: A Case Report and Electronically Captured Patient-Reported Outcome. *Case Reports in Oncology*, *14*(1), 616-621. https://doi.org/10.1159/000513905
32. Shannon, P., Markiel, A., Ozier, O., Baliga, N. S., Wang, J. T., Ramage, D., Amin, N., Schwikowski, B., & Ideker, T. (2003). Cytoscape: A software environment for integrated models of biomolecular interaction networks. *Genome Research*, *13*(11), 2498-2504. https://doi.org/10.1101/gr.1239303
33. Shi, Y. Q., Jin, J., Ji, W. F., & Guan, X. X. (2018). Therapeutic landscape in mutational triple negative breast cancer. *Molecular Cancer*, *17*. https://doi.org/ARTN 9910.1186/s12943-018-0850-9
34. Skov, N., Alves, C. L., Ehmsen, S., & Ditzel, H. J. (2022). Aurora Kinase A and Bcl-xL Inhibition Suppresses Metastasis in Triple-Negative Breast Cancer. *International Journal of Molecular Sciences*, *23*(17). https://doi.org/ARTN 1005310.3390/ijms231710053

35. Sousa da Silva, A. W., & Vranken, W. F. (2012). ACPYPE - AnteChamber PYthon Parser interfacE. *BMC Res Notes*, *5*, 367. https://doi.org/10.1186/1756-0500-5-367

36. Stelzer, G., Rosen, N., Plaschkes, I., Zimmerman, S., Twik, M., Fishilevich, S., Stein, T. I., Nudel, R., Lieder, I., Mazor, Y., Kaplan, S., Dahary, D., Warshawsky, D., Guan-Golan, Y., Kohn, A., Rappaport, N., Safran, M., & Lancet, D. (2016). The GeneCards Suite: From Gene Data Mining to Disease Genome Sequence Analyses. *Curr Protoc Bioinformatics*, *54*, 1 30 31-31 30 33. https://doi.org/10.1002/cpbi.5

37. Sun, S. L., Zhou, W., Li, X. X., Peng, F., Yan, M., Zhan, Y. J., An, F., Li, X. Y., Liu, Y. Y., Liu, Q. T., & Piao, H. Z. (2021). Nuclear Aurora kinase A triggers programmed death-ligand 1-mediated immune suppression by activating MYC transcription in triple-negative breast cancer. *Cancer Communications*, *41*(9), 851-866. https://doi.org/10.1002/cac2.12190

38. Szklarczyk, D., Kirsch, R., Koutrouli, M., Nastou, K., Mehryary, F., Hachilif, R., Gable, A. L., Fang, T., Doncheva, N. T., Pyysalo, S., Bork, P., Jensen, L. J., & von Mering, C. (2023). The STRING database in 2023: protein-protein association networks and functional enrichment analyses for any sequenced genome of interest. *Nucleic Acids Research*, *51*(D1), D638-D646. https://doi.org/10.1093/nar/gkac1000

39. Takchi, A., & Haddad, T. C. (2023). Effect of DUAL pharmacological blockade of AURKA and PD-L1 pathways on plasticity and metastasis for triple negative breast cancer. *Journal of Clinical Oncology*, *41*(16). <Go to ISI>://WOS:001053772001381

40. Takchi, A., Zhang, M. Z., Jalalirad, M., Ferre, R. L., Shrestha, R., Haddad, T., Sarkaria, J., Tuma, A., Carter, J., David, H., Giridhar, K., Wang, L. W., Lange, C., Lendahl, U., Ingle, J., Goetz, M., & D'Assoro, A. B. (2024). Blockade of tumor cell-intrinsic PD-L1 signaling enhances AURKA-targeted therapy in triple negative breast cancer. *Frontiers in Oncology*, *14*. https://doi.org/ARTN 138427710.3389/fonc.2024.1384277

41. Tian, C., Kasavajhala, K., Belfon, K. A. A., Raguette, L., Huang, H., Migues, A. N., Bickel, J., Wang, Y., Pincay, J., Wu, Q., & Simmerling, C. (2020). ff19SB: Amino-Acid-Specific Protein Backbone Parameters Trained against Quantum Mechanics Energy Surfaces in Solution. *Journal of Chemical Theory and Computation*, *16*(1), 528-552. https://doi.org/10.1021/acs.jctc.9b00591

42. Trezza, A., Visibelli, A., Roncaglia, B., Barletta, R., Iannielli, S., Mahboob, L., Spiga, O., & Santucci, A. (2025). Unveiling Dynamic Hotspots in Protein-Ligand Binding: Accelerating Target and Drug Discovery Approaches. *Int J Mol Sci*, *26*(9). https://doi.org/10.3390/ijms26093971

43. Wang, B., Xing, A. Y., Li, G. X., Liu, L., & Xing, C. E. (2024). SNHG14 promotes triple-negative breast cancer cell proliferation, invasion, and chemoresistance by regulating the ERK/MAPK signaling pathway. *Iubmb Life*, *76*(12), 1295-1308. https://doi.org/10.1002/iub.2910

44. Wang, G. J., Duan, P., Wei, Z. K., & Liu, F. (2022). Curcumin sensitizes carboplatin treatment in triple negative breast cancer through reactive oxygen species induced DNA repair pathway. *Molecular Biology Reports*, *49*(4), 3259-3270. https://doi.org/10.1007/s11033-022-07162-1

45. Wang, L. Y., Lu, Q. Y., Jiang, K. K., Hong, R. X., Wang, S. S., & Xu, F. (2022). BRAF V600E Mutation in Triple-Negative Breast Cancer: A Case Report and Literature Review. *Oncology Research and Treatment*, *45*(1-2), 54-60. https://doi.org/10.1159/000520453
46. Wang, S. H., Yeh, C. H., Wu, C. W., Hsu, C. Y., Tsai, E. M., Hung, C. M., Wang, Y. W., & Hsieh, T. H. (2024). PFDN4 as a Prognostic Marker Was Associated with Chemotherapy Resistance through CREBP1/AURKA Pathway in Triple-Negative Breast Cancer. *International Journal of Molecular Sciences*, *25*(7). https://doi.org/ARTN 390610.3390/ijms25073906
47. Zhai, Y., Liu, L., Zhang, F., Chen, X., Wang, H., Zhou, J., Chai, K., Liu, J., Lei, H., Lu, P., Guo, M., Guo, J., & Wu, J. (2025). Network pharmacology: a crucial approach in traditional Chinese medicine research. *Chin Med*, *20*(1), 8. https://doi.org/10.1186/s13020-024-01056-z
48. Zhou, Y., Zhou, B., Pache, L., Chang, M., Khodabakhshi, A. H., Tanaseichuk, O., Benner, C., & Chanda, S. K. (2019). Metascape provides a biologist-oriented resource for the analysis of systems-level datasets. *Nat Commun*, *10*(1), 1523. https://doi.org/10.1038/s41467-019-09234-6
49. Zhu, H. Y., Rao, Z. J., Yuan, S. C., You, J. Q., Hong, C. G., He, Q. J., Yang, B., Du, C. Y., & Cao, J. (2021). One therapeutic approach for triple-negative breast cancer: Checkpoint kinase 1 inhibitor AZD7762 combination with neoadjuvant carboplatin. *European Journal of Pharmacology*, *908*. https://doi.org/ARTN 17436610.1016/j.ejphar.2021.174366
50. Zhu, S. L., Wu, Y. Z., Song, B., Yi, M., Yan, Y. H., Mei, Q., & Wu, K. M. (2023). Recent advances in targeted strategies for triple-negative breast cancer. *Journal of Hematology & Oncology*, *16*(1). https://doi.org/ARTN 10010.1186/s13045-023-01497-3

Figures

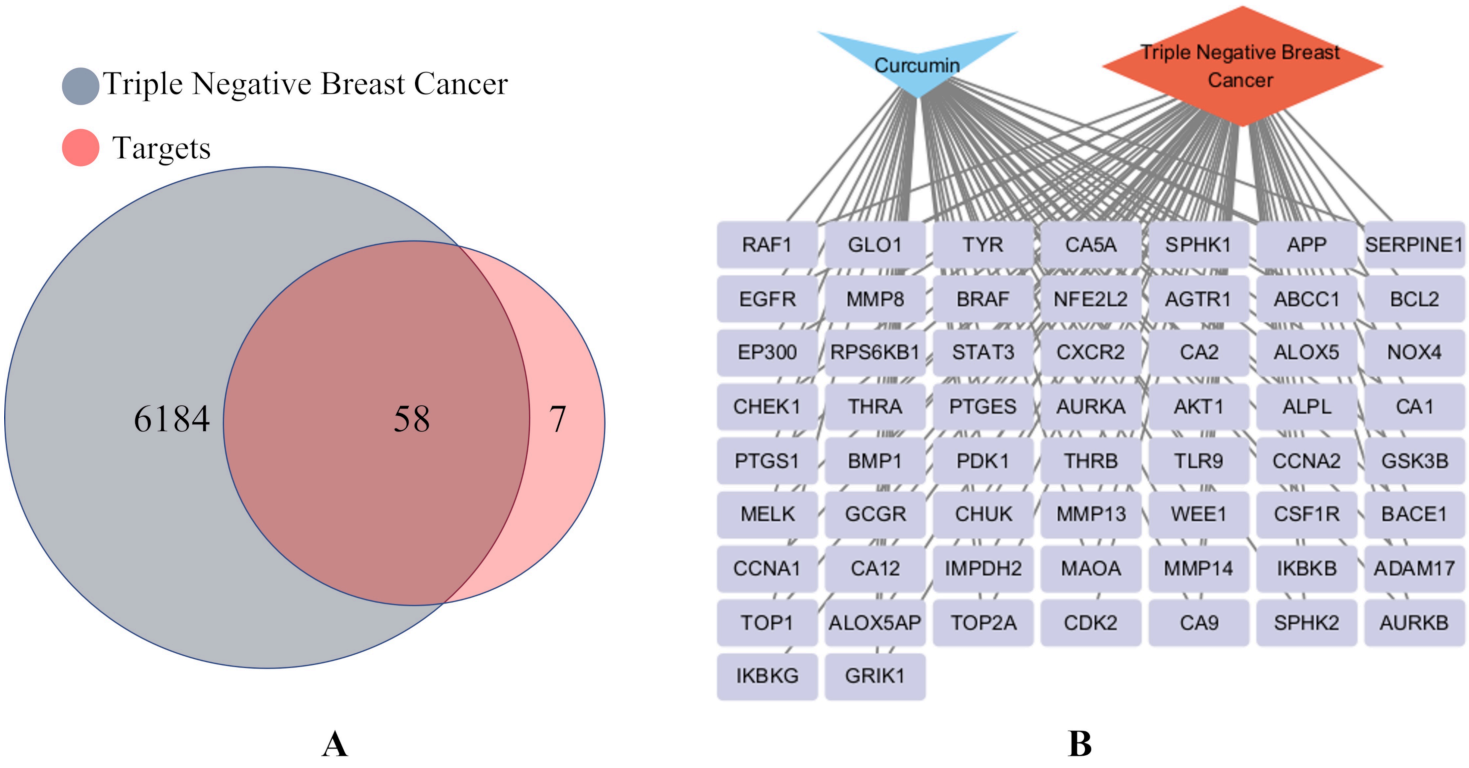

Figure 1

Network pharmacology analysis of curcumin against TNBC.

(A) Venn diagram showing the overlap between 65 predicted and 6282 genes linked to Triple Negative Breast Cancer. 58 targets were found in the investigation.

(B) Traditional Chinese Medicine-active components-target-disease (C–T–D) network of Curcumin (blue node) acting on Triple negative breast cancer (orange node), 58 targets (gray nodes)

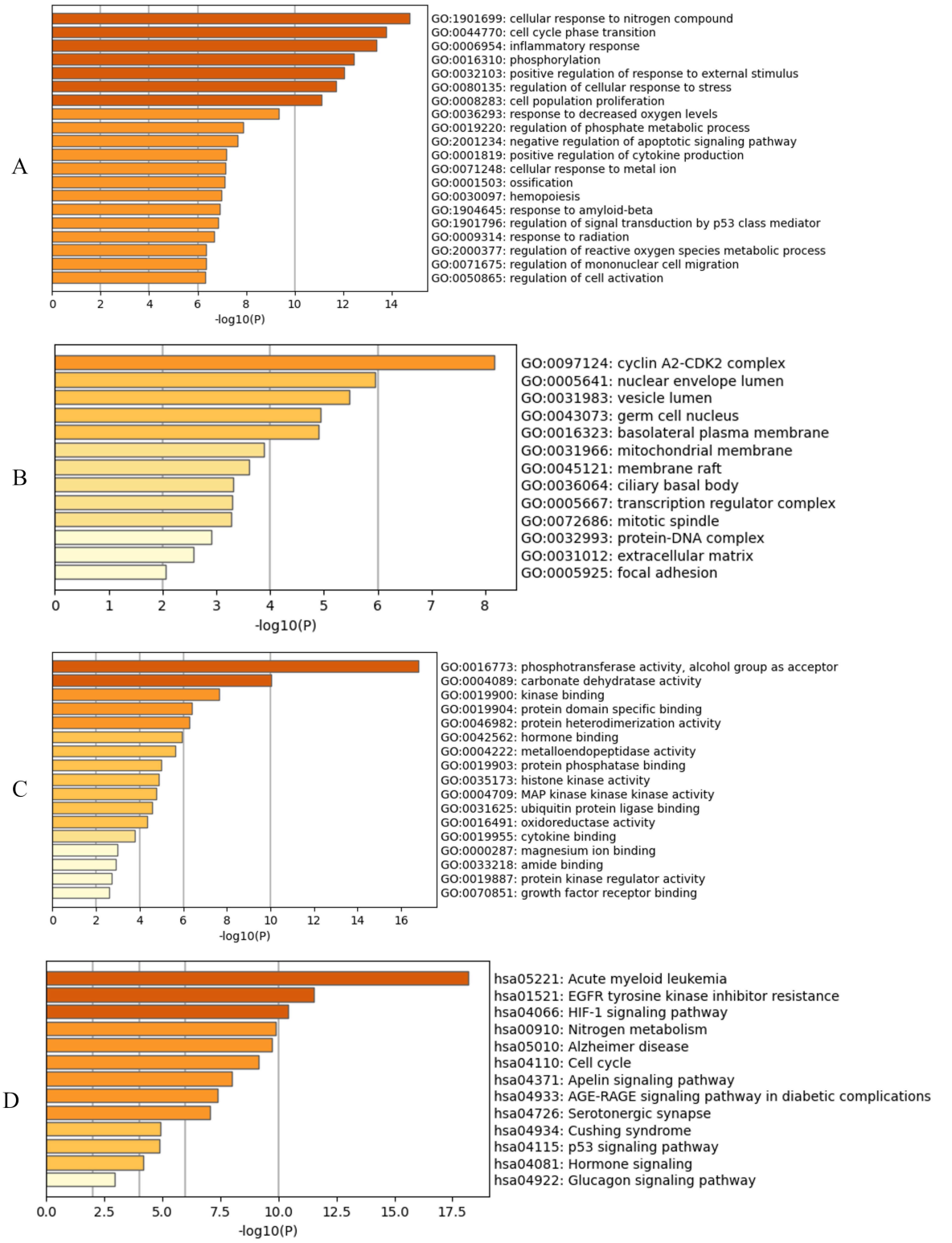

Figure 2

Functional enrichment analysis of overlapping targets between curcumin and TNBC.

(A) Top 20 significantly enriched biological process (BP) terms;

(B) Top 13 cellular component (CC) terms;

(C) Top 13 molecular function (MF) terms;

(D) Top 13 KEGG pathways.

The color scale represents the significance level (−log10 p value), and the length of the bars indicates the number of enriched genes in each category.

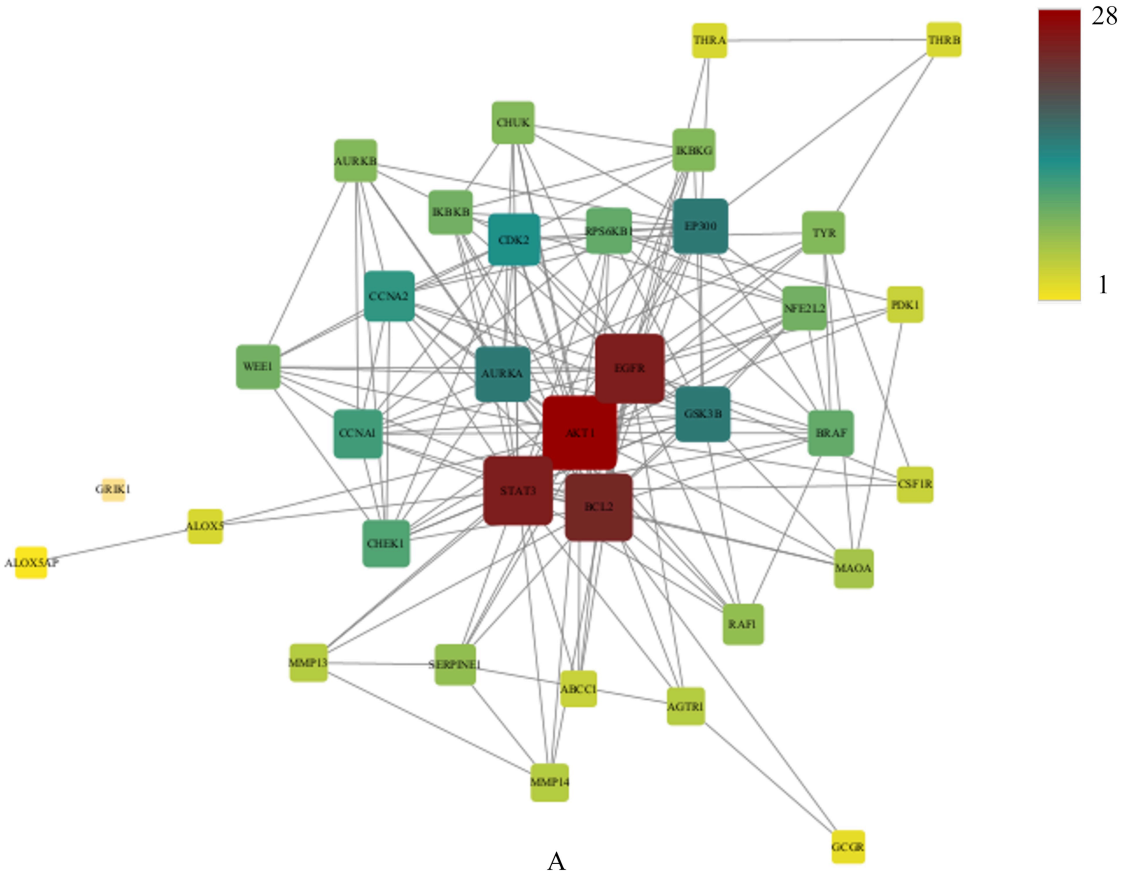

A

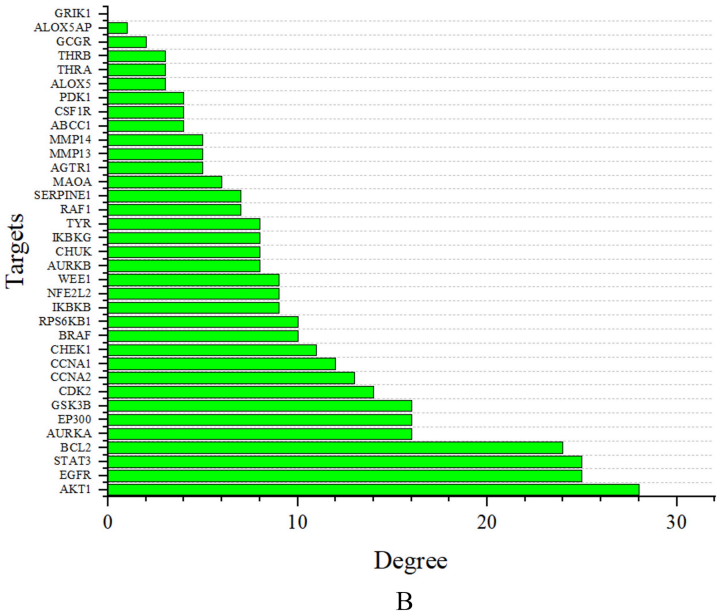

B

Figure 3

Identification of hub genes and protein–protein interaction (PPI) network.

(A) The STRING database was used to create the PPI network of 58 overlapping targets between curcumin and TNBC, which was then displayed in Cytoscape. Proteins are represented by nodes, and protein–protein relationships are represented by edges. The degree value is correlated with node size and color intensity.

(B) A bar graph showing the degree centrality of each PPI network node. hub genes with the highest degree values.

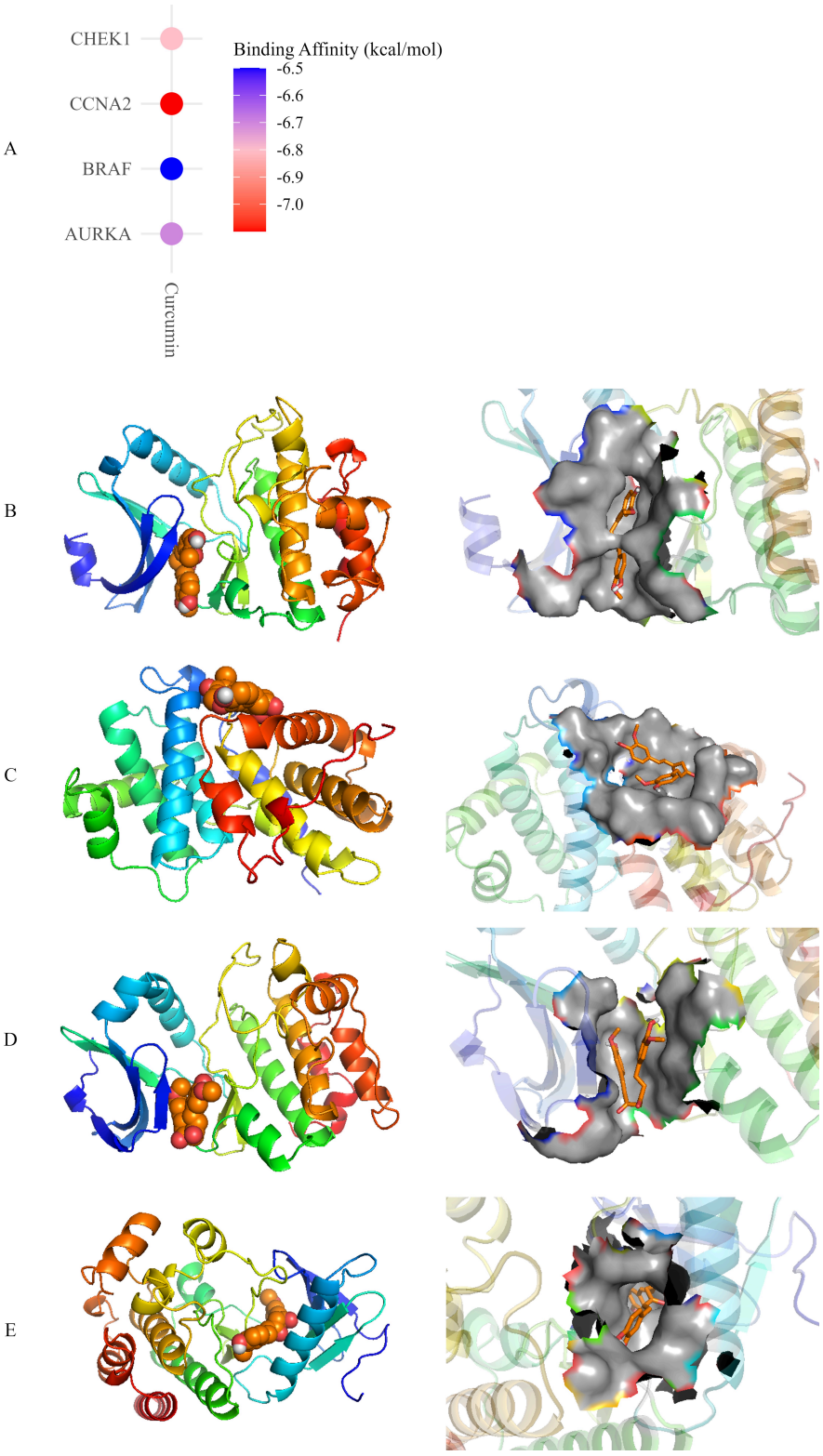

Figure 4

Molecular docking of curcumin with core targets.

(A) AutoDock Vina predicted curcumin's binding affinities (kcal/mol) with AURKA, CCNA2, CHEK1, and BRAF.

(B) Curcumin's docking conformation with CHEK1; the binding pocket's surface is depicted in the right panel.

(C) Curcumin's docking conformation with CCNA2; the binding pocket's surface is depicted in the right panel.

(D) Curcumin's docking conformation with AURKA demonstrates pocket binding; the binding pocket's surface is depicted in the right panel.

(E) Curcumin's docking conformation with BRAF demonstrates pocket binding; the binding pocket's surface is depicted in the right panel.

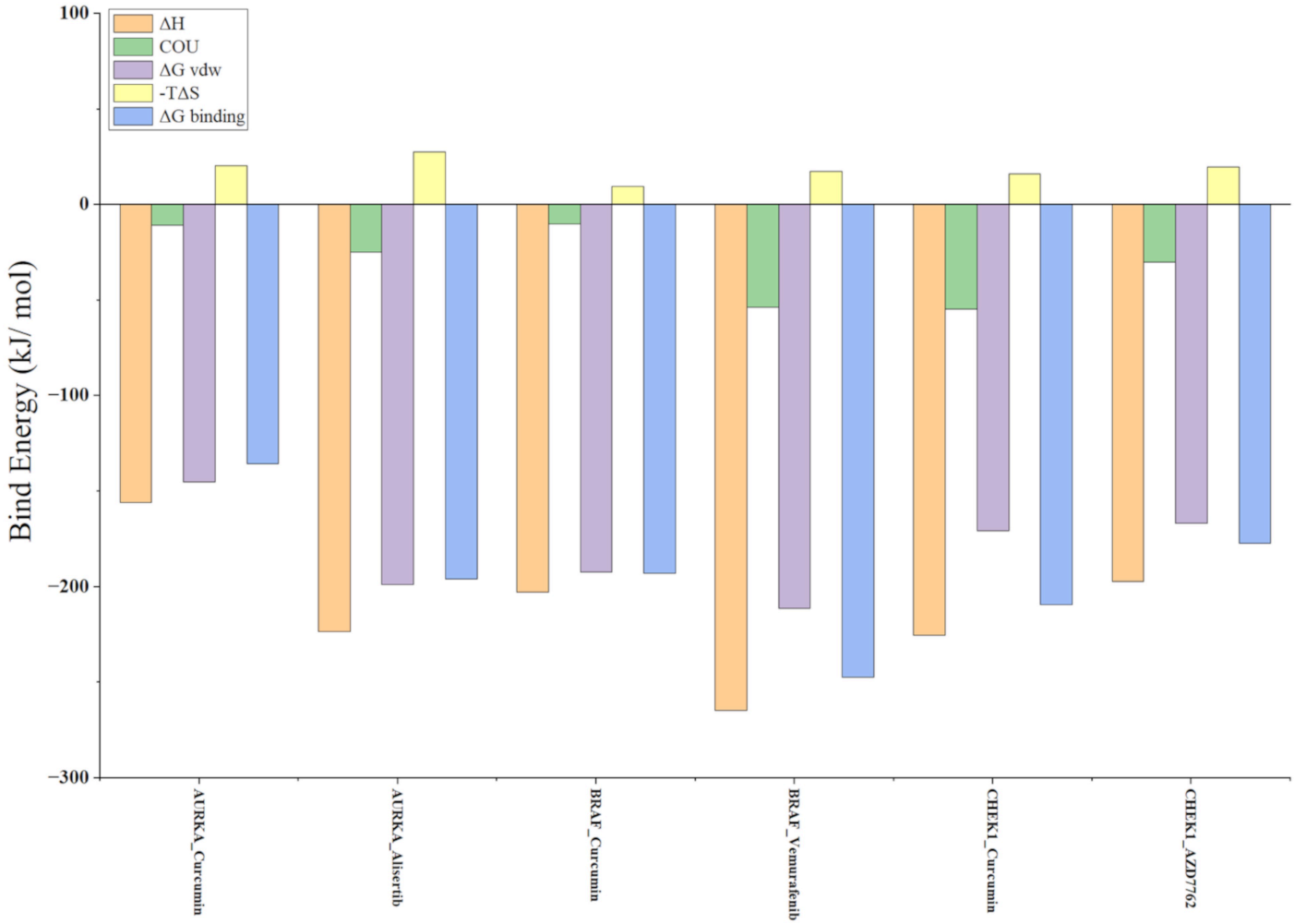

Figure 5

Binding free energy

Curcumin and reference inhibitors (Alisertib, Vemurafenib, and AZD7762) with their respective targets (AURKA, BRAF, and CHEK1) calculated by MM/PBSA.

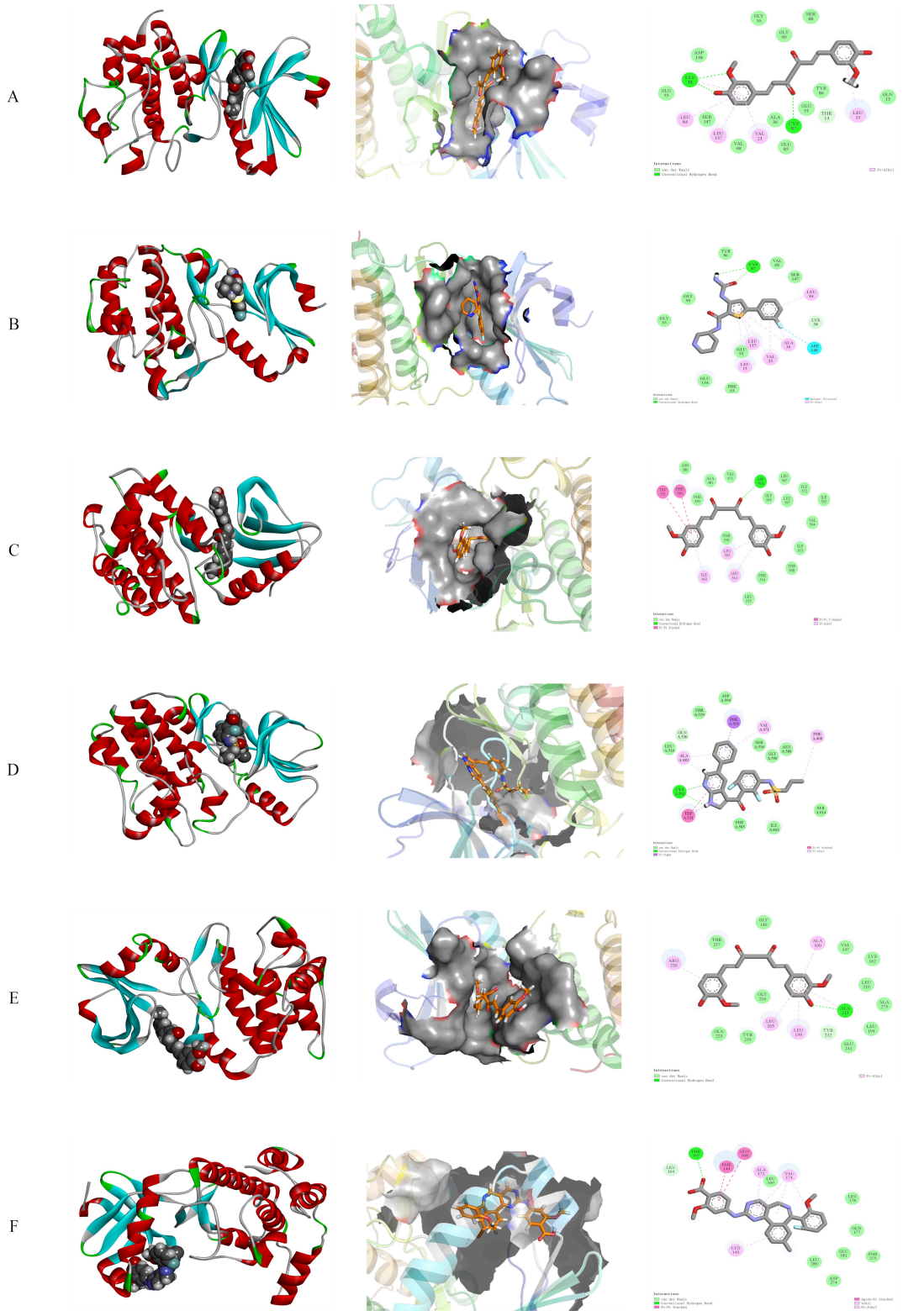

Figure 6

Binding modes of Curcumin and control inhibitors with CHEK1, BRAF, and AURKA proteins.

(A) Curcumin–CHEK1 complex: overall binding position (left), surface pocket view (middle), and 2D interaction diagram (right).

(B) AZD7762–CHEK1 complex: overall structure (left), pocket view (middle), and 2D interaction map (right).

(C) Curcumin–BRAF complex: overall structure (left), pocket view (middle), and 2D interaction map (right).

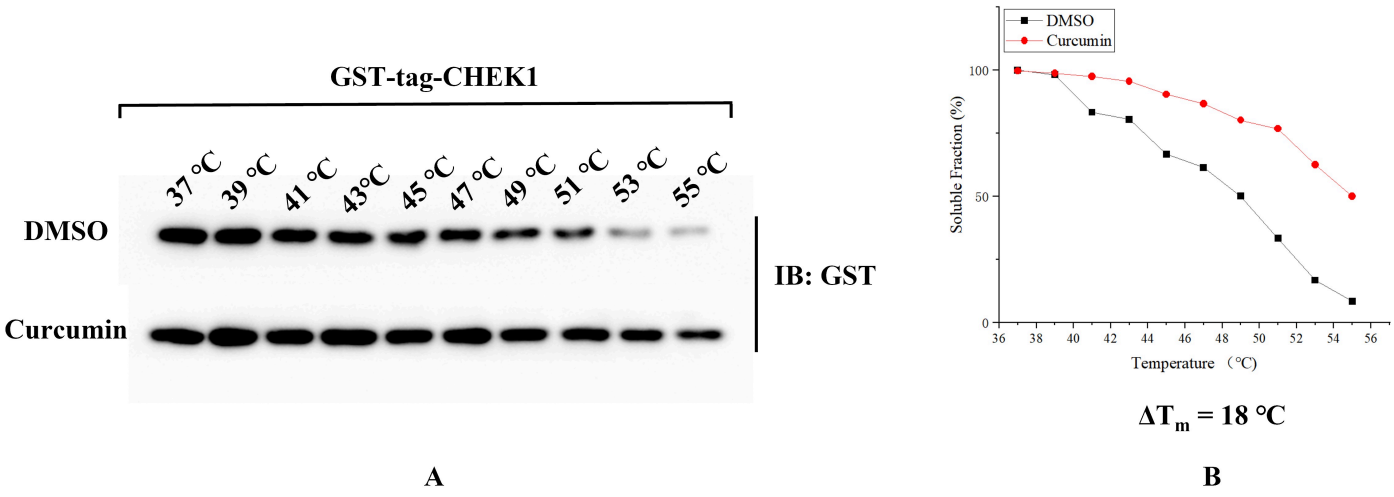

Figure 7

Curcumin can bind to CHEK1.

(A) In vitro thermal shift assay was performed with purified GST-tagged CHEK1 protein in the presence or absence of Curcumin (20 μM), followed by immunoblotting (IB) analysis.

(B) Quantitation and fitting of the data in (A) are shown, along with the ΔTm value.

Supplementary Files

This is a list of supplementary files associated with this preprint. Click to download.

- CTL.tif
- curcumin.tif
- FigureS1.jpg
- FigureS2.jpg
- FigureS3.jpg
- graphicabstract.jpg